Experimental investigation on *Q*-switching and *Q*-switched mode-locking operation in gold nanorods-based erbium-doped fiber laser

Xude Wang (汪徐德)[1,2], Nian Zhao (赵 年)[2], Hao Liu (刘 浩)[2], Rui Tang (汤 瑞)[2], Yanfang Zhu (朱艳芳)[4], Jianping Xue (薛建平)[4], Zhichao Luo (罗智超)[2], Aiping Luo (罗爱平)[2,3,*], and Wencheng Xu (徐文成)[2,]**

[1]*School of Physics and Electronic Information, Huaibei Normal University, Huaibei 235000, China*
[2]*Laboratory of Nanophotonic Functional Materials and Devices, School of Information and Optoelectronic Science and Engineering, South China Normal University, Guangzhou 510006, China*
[3]*Guangdong Provincial Key Laboratory of Fiber Laser Materials and Applied Techniques, South China University of Technology, Guangzhou 510640, China*
[4]*School of Life Sciences, Huaibei Normal University, Huaibei 235000, China*
**Corresponding author: luoaiping@scnu.edu.cn; **corresponding author: xuwch@scnu.edu.cn*
Received March 15, 2015; accepted May 7, 2015; posted online June 11, 2015

We report on the generation of *Q*-switched and *Q*-switched mode-locked (QML) pulses in an erbium-doped fiber ring laser by using a polyvinyl alcohol (PVA) -based gold nanorod (GNR) saturable absorber (SA). The PVA-based GNR SA has a modulation depth of ~4.8% and a non-saturable loss of ~26.9% at 1.5 μm. A *Q*-switched pulse train with a repetition rate varying from 18.70 to 39.85 kHz and a QML pulse train with an envelope repetition rate tuning from 20.31 to 31.50 kHz are obtained. Moreover, the lasing wavelengths of the *Q*-switched pulses can be flexibly tuned by introducing a narrow bandwidth, tunable filter into the laser cavity. The results demonstrate that the GNRs exhibit good optical performance and can find a wide range of applications in the field of laser technology.

OCIS codes: 140.3500, 140.3540, 140.3600, 160.4236.
doi: 10.3788/COL201513.081401.

Fiber lasers capable of generating *Q*-switched and *Q*-switched mode-locked (QML) pulses have attracted considerable attention for their widespread applications, which range from basic research to optical communication, spectroscopy, and material processing that relies on their high-pulse energy output and controllable repetition rate[1,2]. At present, both actively and passively mode-locked techniques have been used to achieve *Q*-switched and QML pulses in fiber lasers. Introducing electro- or acousto-optic modulators enables the actively *Q*-switched fiber laser to attain a tunable and robust repetition rate. However, the cumbersome and complicated laser systems limit their wide range application[3]. On the contrary, passively *Q*-switched fiber lasers have the advantages of compactness and simplicity because they use different kinds of saturable absorbers (SAs). The metal-doped bulk crystal and the semiconductor saturable absorber mirror (SESAM) are the most common SAs used for the passive *Q*-switching operation[4,5]. However, the complex fabrication process and limited operation bandwidth of SESAMs should be taken into consideration. Such limitations motivate research on new materials for SAs. Recently, novel nanomaterials such as the carbon nanotube[6–8], graphene[9–11], and the topological insulator[12–14] have been intensively studied due to their fast recovery time, large third nonlinearity, and broadband saturable absorption characteristics. They show excellent optical performance and good compatibility with the fiber laser, and can be integrated into the cavity to construct a compact, *Q*-switched fiber laser[15–21].

Very recently, gold nanorods (GNRs) have gained particular interest due to the unique features of their surface plasmon resonances (SPRs), which originate from the collective oscillations of the conduction electrons. There are two SPR absorption peaks in the absorption spectrum of GNRs. One is the longitudinal SPR absorption peak, while the other is the transverse one. Interestingly, the position of the longitudinal SPR absorption peak can be widely tuned by varying the aspect ratio of the nanorods, and then can be conveniently shifted to the near-infrared region, which is in the operation waveband of fiber lasers. In addition, the saturable absorption of the longitudinal SPR has been observed with the z-scan technique. The third-order nonlinear optical properties of GNRs have been investigated as well[22,23], suggesting that the GNRs could function as a promising nanomaterial for the fabrication of high-performance SAs. Indeed, by virtue of the advantage of large nonlinearity, picosecond recovery time, and tunable saturable absorption waveband, GNRs are used in fiber laser as SAs for realizing passively *Q*-switched operations[24,25]. To further exploit the potential applications in a GNR-based fiber laser, it is necessary to investigate a wavelength-tunable *Q*-switched operation and a QML operation.

In this Letter, Q-switched and QML pulse outputs from an erbium-doped fiber (EDF) ring laser are investigated by employing GNRs as SAs. A polyvinyl alcohol (PVA) - based GNR SA with a modulation depth of ~4.8% and a non-saturable loss of ~26.9% is obtained at 1.5 μm. The repetition rate of the Q-switched pulse can vary from 18.70 to 39.85 kHz by changing the pump power from 29.7 to 96.3 mW. The envelope repetition rate of the QML pulse trains can be tuned from 20.31 to 31.50 kHz by increasing the pump power from 49.7 to 80 mW. Moreover, the wavelength tunable operation of the Q-switched pulse from 1549.58 to 1558.22 nm has been investigated by introducing a tunable bandpass filter into the cavity. The experimental results indicate that GNRs are indeed a good candidate for the ultrafast saturable absorption device in pulsed fiber lasers.

The GNRs was synthesized by the high-efficiency, modified seed-mediated method, similar to our previous work in Ref. [26]. The obtained GNRs were purified by centrifuging them twice at 10000 rpm for 15 min. the fabricated GNRs were prepared by removing the supernatant and re-dispersing the precipitate in ultrapure water. The structure of the GNRs was observed by a transmission electron microscope (TEM, JEM-2100), as shown in Fig. 1(a). From the images, a large quantity of GNRs with some nanoparticle byproducts can be clearly seen. The average diameter is ~17.2 nm. The inset of Fig. 1(a) presents the as-synthesized aqueous solution of the GNRs, which has a purplish red color. Figure 1(b) illustrates the histogram of the aspect ratio distribution of the GNRs. The aspect ratio of the GNRs varies from 5.5 to 13.5, indicating that the GNRs have broadband absorption that will cover the 1550 nm waveband according to the method of discrete dipole approximation[27].

The PVA-based GNR SA is prepared by mixing aqueous dispersion of GNRs and the PVA solution, as reported in Ref. [14]. The filmy GNR SA is formed at room temperature on a slide glass. With the help of the deionized water, which was dripped on the fiber's end face, the small film could be easily transferred to the end face of the optical fiber, as shown in Fig. 2(a). To get further insight into the optical properties of the GNRs film, the saturable absorption of the PVA-based GNRs SA was characterized by a balanced twin detector measurement technology[28]. Figure 2(b) provides the saturable absorption data of the GNR SA. The modulation depth and the non-saturable loss are ~4.8% and ~26.9%, respectively. The saturable absorption phenomenon of the GNRs could be derived from the conduction band transition of the s-p electron, which induces bleaching in the ground-state plasmon absorption[22,29].

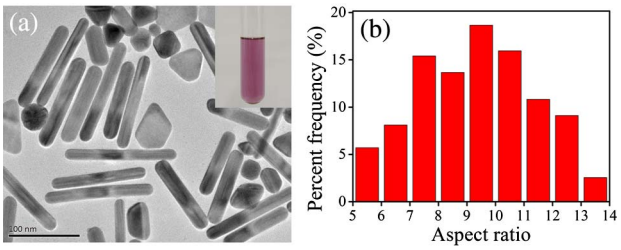

Fig. 1. (a) TEM image of the GNRs (Inset: aqueous solution of GNRs). (b) Histogram of the aspect ratio distribution.

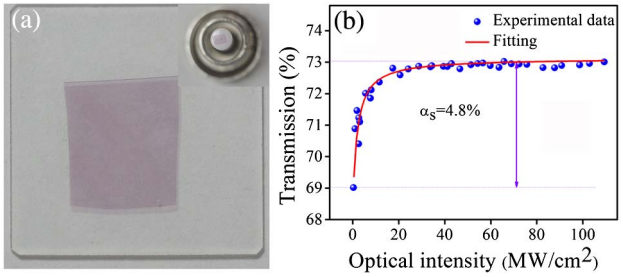

Fig. 2. (a) Photograph of the filmy GNR SA (Inset: photograph of the fiber end attached to the GNR SA). (b) Nonlinear saturable absorption curve of the prepared GNR SA.

The schematic of the proposed Q-switched EDF laser is shown in Fig. 3. A 4.8 m long EDF is used as the gain medium and is pumped by a 980 nm laser diode via a 980/1550 nm wavelength division multiplexer. The polarization state of the circulating light in the laser cavity can be controlled by two polarization controllers (PCs). In order to ensure a unidirectional operation, a polarization insensitive isolator was employed. The prepared GNR SA was sandwiched between the optical fiber connectors so that it could modulate the optics circulating in the fiber laser. The total laser cavity length is ~51.4 m, corresponding to the repetition rate of ~4 MHz The output laser emission is taken by a 10/90 coupler. An oscilloscope, together with a photodetector and an optical spectrum analyzer, are used to analyze the temporal and spectral properties of the output signal.

Firstly, the GNR SA was not spliced in the laser cavity. In this case, no Q-switched operation could be observed. In contrast, when the GNR SA was incorporated into the cavity, the Q-switched pulse occurred at a pump power of 27.6 mW with the proper setting of the PCs, confirming that the saturable absorption of the GNR film had been activated to initiate the Q-switching. Figure 4 shows the characteristics of a typical Q-switched operation at a pump power of 56.4 mW. As is shown in Fig. 4(a), the

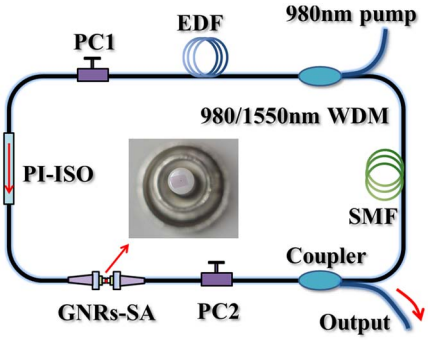

Fig. 3. Experimental setup of Q-switched EDF ring laser.

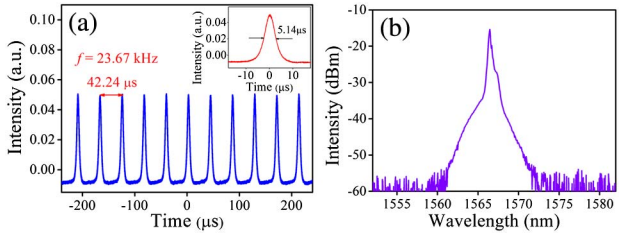

Fig. 4. Q-switched operation at a pump power of 56.4 mW. (a) Q-switched pulse train (Inset: the single zoomed-in pulse). (b) The corresponding optical spectrum.

pulse train has the repetition rate of 23.67 kHz, which corresponds to a time interval of 42.24 μs. The zoomed-in view of the single Q-switched pulse profile is presented in the inset of Fig. 4(a), which shows a pulse width of ~5.14 μs. Figure 4(b) shows the corresponding optical spectrum with the central wavelength of 1566.5 nm.

Then, we investigate the Q-switched pulse evolution with varying pump powers at fixed PCs setting. As illustrated in Fig. 5(a), the time interval between the adjacent Q-switched pulses becomes narrower with the increased pump power. The repetition rate of the pulse train is increased from 18.70 to 39.85 kHz when the pump power varies from 34.4 to 96.3 mW. Figure 5(b) shows the measured temporal width and repetition rate of the Q-switched pulses versus the pump power. It should be noted that the pulse duration first decreases and subsequently increases. The minimum pulse duration is ~4.53 μs at a pump power of 74.2 mW, which might be a sign that the Q-switching is changing to another operational state[30]. It is worth mentioning that the pulse duration could be further shortened by reducing the length of the laser cavity[31]. These results coincide well with the inherent features of the Q-switched fiber laser.

To obtain the wavelength tunable Q-switched operation, a tunable bandpass filter with a bandwidth of 0.9 nm is introduced into the cavity to select the lasing wavelength. Since the tunable filter brings a large insertion loss and limits the spectral bandwidth, the Q-switched threshold is increased up to 132.4 mW. Then, in the following experiment, we fix the pump power at the proper value of 202.2 mW and continuously tune the transmission wavelength of the filter with the fixed PC settings. Figure 6(a) presents the spectrum of the wavelength-tunable Q-switched operation. The central wavelength

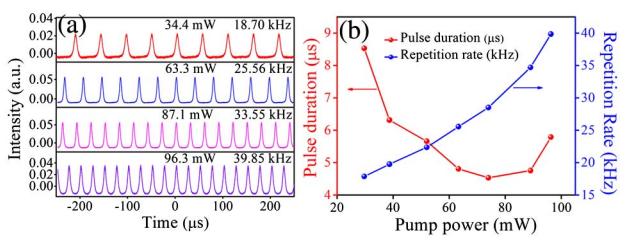

Fig. 5. (a) Q-switched pulse trains with different repetition rates. (b) Pulse duration and repetition rate versus pump power.

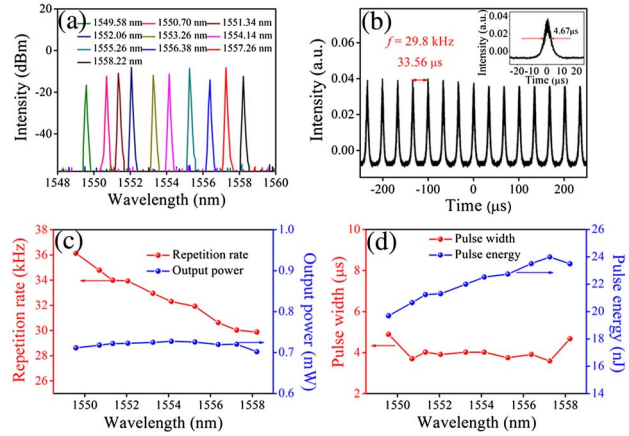

Fig. 6. (a) Spectra of the wavelength-tunable, Q-switched operation at a pump power of 202.2 mW. (b) Typical Q-switched pulses centered at 1558.22 nm. (c) Pulse repetition rate and output power versus tunable wavelength. (d) Pulse width and energy versus tunable wavelength.

can vary from 1549.58 to 1558.22 nm, and the Q-switched operation remains stable in the process of tuning. The variations in the spectral intensities can probably be ascribed to the difference between the cavity loss and the gain effect of the EDF at different wavelengths[1,32]. Figure 6(b) shows the typical Q-switched pulses centered at 1558.22 nm. A single pulse with a duration of ~4.67 μs is shown in the inset of Fig. 6(b). The dependent relations of the repetition rate, average output power, the pulse duration, and the energy of Q-switched pulses with respect to the different central wavelengths are presented in Figs. 6(c) and 6(d). When the central wavelength shifts from a short wavelength (1549.58 nm) to a long wavelength (1558.22 nm), the repetition rate decreases gradually from 36.13 to 29.88 kHz, and the pulse energy increases almost linearly from 19.69 to 23.49 nJ. The output power fluctuation is insignificant; it reaches the maximum value of 0.73 mW at 1554.14 nm, and the pulse width fluctuates around 4 μs during the wavelength tuning process. In this experiment, the tuning range of the Q-switched operation could be limited by the saturable absorption bandwidth of the GNR-based SA. One further improvement could be made by mixing the GNRs with different aspect ratios, which might enable the GNRs to create a broadband SA.

With the proper setting of the PCs and the proper pump power, the state of the Q-switching operation could be evolved into a QML operation in the laser cavity. The pulse of the QML is uniformly sequenced in a train and displays a large Q-switched envelope, which appears on top of the mode-locked pulses. Figure 7(a) shows the different repetition rates of the QML pulse trains under different pump powers. As can be seen, the envelope repetition rate of the QML pulse trains can be tuned from 20.31 to 31.50 kHz when the pump power increases from 49.7 to 80 mW. Figure 7(b) shows the typical zoomed-in image of the QML pulse that is shown in Fig. 7(a). It can be clearly seen that a train of laser pulses is contained in

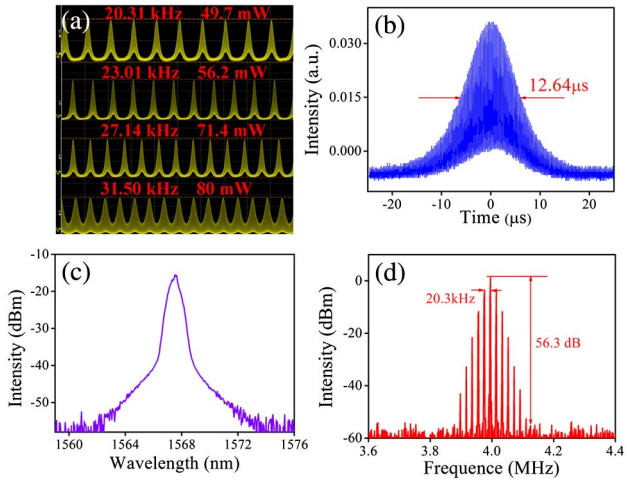

Fig. 7. (a) Various QML pulse trains under different pump powers. (b) Magnified view of the single QML pulse. (c) The corresponding optical spectrum. (d) The corresponding radio frequency spectrum.

the Q-switching envelope. The temporal width of the Q-switched envelope is ~12.64 μs, and the time interval between the internal pulses is ~250 ns. The corresponding optical spectrum can be seen in Fig. 7(c). The central wavelength of the QML pulses is 1567.6 nm with a 3 dB bandwidth of 0.68 nm. To investigate the stability of the QML pulses in detail, the radio frequency spectrum is measured, as presented in Fig. 7(d). A central frequency peak along with many side frequency components occurred in the radio frequency spectrometer. The central peak with a signal-to-noise ratio of ~56 dB is located at 4.0 MHz, which corresponds to the fundamental repetition rate of mode locked pulses. The frequency offset between the adjacent side frequency components is 20.3 kHz, corresponding to the repetition rate of the Q-switched envelope. This electrical spectrum indicates that an amplitude modulation at a frequency of 20.3 kHz is imposed onto the continuous 4.0 MHz mode-locked pulse train[33]. The observation confirms that the SA provides the required mechanism to initiate and sustain a Q-switched mode-locking operation in which the GNR SA is the key component. Note that the switching between operation states depends on the pulse energy under the control of the PCs and pump power. Therefore, if the intra-cavity pulse energy gets close to the switching threshold, the fiber laser could switch to the QML regime[34]. Hence, with the proper setting of the PCs and pump power, the transition from Q-switching to a QML operation is realized.

In conclusion, we demonstrate a filmy GNR SA-based, passively Q-switched and QML EDF laser. The PVA-based GNR SA is confirmed to show a modulation depth of ~4.8% and a non-saturable loss of ~26.9% at 1.5 μm. Moreover, the tunable repetition rate of the Q-switched and the QML are obtained under different pump powers. By introducing a tunable bandpass filter into the cavity, the wavelength tunable operation of the Q-switched pulses is also achieved. The results of our experiment indicate that GNRs exhibit good optical performance and have potential applications in pulsed fiber lasers.

This work was supported by the National Natural Science Foundation of China (Grant Nos. 61378036, 61307058, 11304101, 11074078, and 11474108), the PhD Start-Up Fund of the Natural Science Foundation of Guangdong Province, China (Grant No. S2013040016320), the Scientific Research Foundation of the Graduate School of South China Normal University, China (Grant No. 2014bsxm06), the Zhujiang New-Star Plan of Science and Technology in Guangzhou City (Grant No. 2014J2200008), and the Open Fund of the Guangdong Provincial Key Laboratory of Fiber Laser Materials and Applied Techniques (South China University of Technology).

References

1. Y. Chen, C. J. Zhao, S. Q. Chen, J. Du, P. H. Tang, G. B. Jiang, H. Zhang, S. C. Wen, and D. Y. Tang, IEEE J. Sel. Topics Quantum Electron. **20**, 0900508 (2014).
2. Z. T. Wang, S. E. Zhu, Y. Chen, M. Wu, C. J. Zhao, H. Zhang, G. C. A. M. Janssen, and S. C. Wen, Opt. Commun. **300**, 17 (2013).
3. M. V. Andrés, J. L. Cruz, A. Díez, P. Pérez-Millán, and M. Delgado-Pinar, Laser Phy. Lett. **5**, 93 (2007).
4. M. Laroche, A. M. Chardon, J. Nilsson, D. P. Shepherd, W. A. Clarkson, S. Girard, and R. Moncorgé, Opt. Lett. **27**, 1980 (2002).
5. J. Y. Huang, S. C. Huang, H. L. Chang, K. W. Su, Y. F. Chen, and K. F. Huang, Opt. Express **16**, 3002 (2008).
6. S. Yamashita, Y. Inoue, S. Maruyama, Y. Murakami, H. Yaguchi, M. Jablonski, and S. Y. Set, Opt. Lett. **29**, 1581 (2004).
7. X. M. Liu, D. D. Han, Z. P. Sun, C. Zeng, H. Lu, D. Mao, Y. D. Cui, and F. Q. Wang, Sci. Rep. **3**, 2718 (2013).
8. X. H. Li, Y. G. Wang, Y. S. Wang, W. Zhao, W. C. Yu, Z. P. Sun, X. P. Cheng, X. Yu, Y. Zhang, and Q. J. Wang, Opt. Express **22**, 17227 (2014).
9. Z. P. Sun, T. Hasan, F. Torrisi, D. Popa, G. Privitera, F. Wang, F. Bonaccorso, D. M. Basko, and A. C. Ferrari, ACS Nano **4**, 803 (2010).
10. H. Zhang, D. Y. Tang, R. J. Knize, L. M. Zhao, Q. L. Bao, and K. P. Loh, Appl. Phys. Lett. **96**, 111112 (2010).
11. Y. Chen, C. J. Zhao, Z. T. Wang, J. C. Song, H. Zhang, and S. C. Wen, Opt. Eng. **51**, 084203 (2012).
12. C. J. Zhao, H. Zhang, X. Qi, Y. Chen, Z. T. Wang, S. C. Wen, and D. Y. Tang, Appl. Phys. Lett. **101**, 211106 (2012).
13. P. G. Yan, R. Y. Lin, H. Chen, H. Zhang, A. J. Liu, H. P. Yang, and S. C. Ruan, IEEE Photon. Technol. Lett. **27**, 951 (2015).
14. H. Liu, X. W. Zheng, M. Liu, N. Zhao, A. P. Luo, Z. C. Luo, W. C. Xu, H. Zhang, C. J. Zhao, and S. C. Wen, Opt. Express **22**, 6868 (2014).
15. D. P. Zhou, L. Wei, B. Dong, and W. K. Liu, IEEE Photon. Technol. Lett. **22**, 9 (2010).
16. Z. Q. Luo, M. Zhou, J. Weng, G. M. Huang, H. Y. Xu, C. C. Ye, and Z. P. Cai, Opt. Lett. **35**, 3709 (2010).
17. Z. Q. Luo, Y. Z. Huang, J. Weng, H. H. Cheng, Z. Q. Lin, Z. P. Cai, and H. Y. Xu, Opt. Express **21**, 29516 (2013).
18. Z. Y. Dou, Y. R. Song, J. R. Tian, Z. Y. Dou, H. Y. Guoyu, K. X. Li, H. W. Li, and X. P. Zhang, Opt. Express **22**, 24055 (2014).

19. Z. Q. Luo, C. Liu, Y. Z. Huang, D. D. Wu, J. Y. Wu, H. Y. Xu, Z. P. Cai, Z. Q. Lin, L. P. Sun, and J. Weng, IEEE J. Sel. Topics Quantum Electron. **20**, 0902708 (2014).
20. R. Z. R. R. Rosdin, F. Ahmad, N. M. Ali, S. W. Harun, and H. Arof, Chin. Opt. Lett. **12**, 091404 (2014).
21. N. Kasim, A. H. H. Al-Masoodi, F. Ahmad, Y. Munajat, H. Ahmad, and S. W. Harun, Chin. Opt. Lett. **12**, 031403 (2014).
22. H. I. Elim, J. Yang, J. Y. Lee, J. Mi, and W. Ji, Appl. Phy. Lett. **88**, 083107 (2006).
23. O. B. Joanna, G. Marta, K. Radoslaw, M. Katarzyna, and S. Marek, J. Phys. Chem. C **116**, 13731 (2012).
24. Z. Kang, X. Y. Guo, Z. X. Jia, Y. Xu, L. Liu, D. Zhao, G. S. Qin, and W. P. Qin, Opt. Mater. Exp. **3**, 1986 (2013).
25. T. Jiang, Y. Xu, Q. J. Tian, L. Liu, Z. Kang, R. Y. Yang, G. S. Qin, and W. P. Qin, Appl. Phys. Lett. **101**, 151122 (2012).
26. X. D. Wang, Z. C. Luo, H. Liu, M. Liu, A. P. Luo, and W. C. Xu, Appl. Phys. Lett. **105**, 161107 (2014).
27. A. Brioude, X. C. Jiang, and M. P. Pileni, J. Phys. Chem. B **109**, 13138 (2005).
28. Z. C. Luo, M. Liu, H. Liu, X. W. Zheng, A. P. Luo, C. J. Zhao, H. Zhang, S. C. Wen, and W. C. Xu, Opt. Lett. **38**, 5212 (2013).
29. R. Wang, Y. Wang, D. Han, C. Zheng, J. Leng, and H. Yang, Chin. Opt. Lett. **10**, 101902 (2012).
30. J. Lee, J. Koo, Y. M. Chang, P. Debnath, Y. W. Song, and J. H. Lee, J. Opt. Soc. Am. B **29**, 1479 (2012).
31. J. J. Degnan, IEEE J. Quant. Electron. **31**, 1890 (1995).
32. W. J. Cao, H. Y. Wang, A. P. Luo, Z. C. Luo, and W. C. Xu, Laser Phys. Lett. **9**, 54 (2012).
33. Y. M. Chang, J. Lee, and J. H. Lee, Opt. Express **19**, 26627 (2011).
34. K. H. Lin, J. J. Kang, H. H. Wu, C. K. Lee, and G. R. Lin, Opt. Express **17**, 4806 (2009).